

NUMERICAL MODELING OF MAGNETIC DRUG TARGETING

P. Kopcansky^a, *M. Timko*^a, *M. Hnatic*^a, *M. Vala*^{a,b},
G. M. Arzumanyan^b, *E. A. Hayryan*^b, *L. Jancurova*^{b,c}, *J. Jadlovsky*^c

^a Institute of Experimental Physics, Košice, Slovakia

^b Joint Institute for Nuclear Research, Dubna

^c Technical University, Košice, Slovakia

A special focused magnet, designed for the use in the magnetic targeted drug delivery system, was constructed. The theoretical calculation of the adhesion condition for a magnetic fluid drop in magnetic field with obtained design showed that the constructed focused magnet generates a sufficient magnetic force for the capture of a magnetic drop on the vessel wall and can be used 1.5–2 cm deeper in an organism compared with the prism permanent magnet, which can enable non-invasivity of the magnetic drug targeting procedure. The maximal values for magnetic field and gradient of magnetic field are 0.38 T and 101 T/m, respectively.

Построен специально сфокусированный магнит, предназначенный для доставки магнитных лекарственных препаратов. Теоретический анализ условия адгезии магнитной капли в магнитном поле разработанного магнита показал, что последний генерирует достаточную магнитную силу для захвата магнитной капли на стенке сосуда, проникающую на 1,5–2 см глубже в организм по сравнению с магнитным полем постоянного магнита, что позволяет бесконтактно доставлять магнитный лекарственный препарат. Максимальные значения для магнитного поля и градиента магнитного поля 0,38 Тл и 101 Тл/м соответственно.

PACS: 47.63.mh

The difference between success and failure of chemotherapy depends not only on the drug itself but also on how it is delivered to its target. One of the major problems in pharmacotherapy is the delivery of drugs to a specific location and maintenance of its location for the desired length of time. Because of the relatively nonspecific action of chemotherapeutic agents, there is almost always some toxicity to normal tissues. Therefore, it is of great importance to be able to selectively target the magnetically labelled drug to the tumor target as precisely as possible, to reduce resulting systemic toxic side effects from generalized systemic distribution and to be able to use a much smaller dose, which would further lead to a reduction of toxicity. The method of magnetic drug targeting is dependent on physical properties, concentration and amount of applied nanoparticles, on type of binding of the drugs, on the physiological parameters of the patient and of course on magnetic force, which is defined by its field and field gradient [1]. Guided transport of biologically active substances to the target organ allows creating an optimum therapeutic concentration of the drug in the desired part of organism, while keeping the total injected dose low [2–4]. Current research on methods to target chemotherapy drugs in the human body includes the investigation

of biocompatible magnetic nano-carrier systems, e.g., magnetic liquids such as ferrofluids. The use of biocompatible magnetic fluid as potential drug carrier appears to be a promising technique. Due to their superparamagnetic properties, the magnetic fluid drops can be precisely transported, positioned and controlled in desirable parts of blood vessels or hollow organs with the help of an external magnetic field. The motion of magnetic drop within the body is controlled by the combination of magnetic force and a hemodynamic drag force due to blood flow. The models which investigate the interaction of an external magnetic field with blood flow containing a magnetic carrier substance are based on the Maxwell and Navier–Stokes equations, where a static magnetic field is coupled to fluid flow. This is achieved by adding a magnetic volume force to the Navier–Stokes equations, which stems from the solution of magnetic field problem [5]. In order to effectively overcome the influence of blood flow the magnetic force must be larger than the drag force. The conditions for holding a magnetic fluid drop on a blood vessel wall were investigated by Voltairas et al. [6]. In this work the nonuniformity of considered magnetic field is higher only close to the magnetic pole, what was regarded as a major technical problem that has to be resolved in order for the drug targeting to remain essentially non-invasive. The aim of our work was to construct a focused magnet, which enables one to achieve maximal magnetic force in deeper position, to map its magnetic field and to find the adhesion condition for a magnetic fluid drop in magnetic field with obtained design.

Voltairas et al. [6] presented a self-consistent ferrohydrodynamic theory of magnetic drug targeting and examined a model case to account for adhesion. They obtained an upper bound of the mean blood flow velocity as a function of the applied magnetic field, which was considered to be produced by a point source located outside the body at $x = -\delta$, $y = 0$, $z = \zeta$ ($\delta, \zeta > 0$, nonuniformity higher only close to magnetic pole) and had the form

$$\mathbf{H} = \frac{m(\mathbf{r} + \delta\hat{e}_x - \zeta\hat{e}_z)}{(r^2 + \delta^2 + \zeta^2 + 2\delta x - 2\zeta z)^{3/2}}, \quad (1)$$

where m is the magnetic dipole moment. The magnetic point source was oriented at an angle

$$\omega = \arcsin\left(\frac{\zeta}{\delta}\right) \quad (2)$$

with respect to the x axis. Thus, instead of one adhesion condition, Voltairas et al. [6] obtained two equations (3) and (4), and the dependence of blood flow velocity on the applied magnetic field was parameterized as

$$B_m = B_m(R\delta, \chi, \omega) \quad (3)$$

and

$$V_m = V_m(R\delta, \chi, \omega, \gamma_0). \quad (4)$$

The obtained law $V_m = V_m(B_m)$ gives an upper bound of the mean blood flow velocity, at which the applied magnetic field is able to capture a magnetic drug drop on the blood vessel wall. The used magnetic field geometry does not give sufficient magnetic field and magnetic field gradient to apply this magnet in deeper position in organism, therefore we used concept of focusing of magnetic field to achieve better results for magnetic drug targeting.

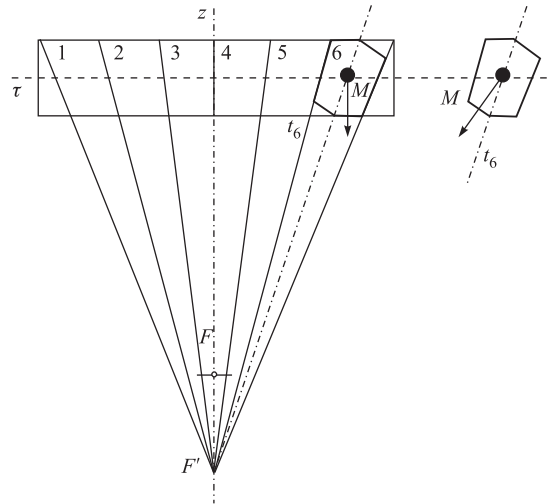


Fig. 1. The cross section of the focused magnet

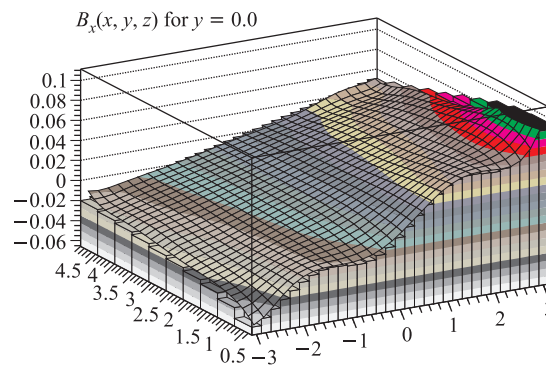


Fig. 2. The x components of magnetic field as a function of x, z for $y = 0.0$

The proposed magnetic system is given in Fig. 1. To construct the map of magnetic field is not very easy task and for this we used GRID computing.

Consecutively we have tested the constructed magnet from the point of magnetic field induction and magnetic field gradient, respectively. The magnetic field of the manufactured focused magnet was measured by 3D Hall probe. The maximal value of the magnetic field near the magnet surface (0.35 mm) was estimated to be 0.38 T. For example, the magnetic field gradient at $z = 0$ was estimated to be 101 T/m. The measured magnetic field by Hall probe was used for the construction of a map of the magnetic field of the focused magnet. The examples of all componets of magnetic field, i.e., $B_x(x, y, z)$, $B_y(x, y, z)$, $B_z(x, y, z)$, are illustrated in Figs.2–4 (for $y = 0.0$). As an example, the function used for fitting of magnetic field $B_x(x, y, z)$ is given in Appendix.

In effort to test the ability of the magnet to generate a strong magnetic field in deeper position, the found profile of its magnetic field was used in the numerical calculation following

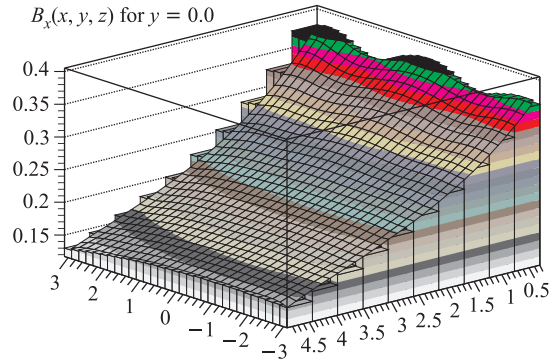


Fig. 3. The y components of magnetic field as a function of x, z for $y = 0.0$

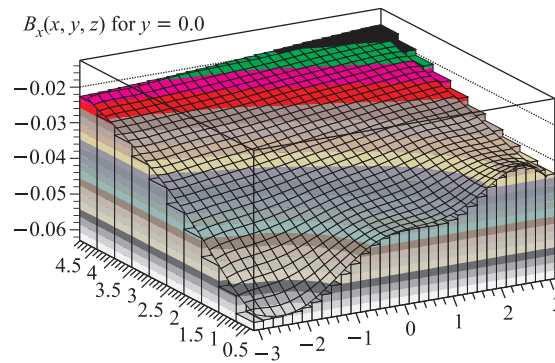


Fig. 4. The z components of magnetic field as a function of x, z for $y = 0.0$

the Voltairas et al. model. The aim was to find the parameters for which the dependence B_m vs. V_m fits the curves obtained in [6]. The results are given in the table.

In summary, a focused magnet consisting of 36 prisms with pyramidal shape was manufactured, generating higher magnetic field and higher magnetic field gradient as compared with classical prism. The magnetic field of the focused magnet was mapped and its profile was used in numerical calculations, which yielded the upper bound of the mean blood flow velocity, at which the applied magnetic field is able to capture a magnetic drug drop on the blood vessel wall. The obtained results verified the ability of the magnet to generate a sufficient magnetic force in deeper position (2.5–3 cm), which could contribute to the non-invasivity of the magnetic drug targeting procedure.

Parameters	Femoral artery $RI\delta \approx 0$	Carotid artery $R/\delta \approx 0.2$
B_0 , T	0.195	0.234
u_0 , ms (computed)	0.462	0.841
u_{exp} , ms (experiment)	0.05–0.35	0.1–0.6
F_m , kN/m ³	5.992	105.025
dB/dx , T/m	7.747	107.824
M , mT	0.975	1.170

Acknowledgements. This work was supported by the Project of ERA NET MAFINCO and in the framework of the Project of Structural Funds of EU-Centrum Excellence: Cooperative Phenomena and Phase Transitions in Nanosystem with perspective utilization in Technics and Biomedicine No.26220120021 and Centre of Excellence of Power Electronics Systems and Materials for their components No.26220120003 which is funded by European Community, ERDF — European Regional Development Fund and JINR Dubna, protocol No.33920-06-09/10. This work was supported by the Russian Foundation for Basic Research (Projects 10-01-00467, 08-01-00800).

APPENDIX

$$\begin{aligned}
 & c_0 + c_1x + c_2y + c_3z + c_4x^2 + c_5y^2 + c_6z^2 + c_7xy + c_8yz + c_9zx + c_{10}x^3 + c_{11}y^3 + c_{12}z^3 + \\
 & c_{13}x^2y + c_{14}xy^2 + c_{15}y^2z + c_{16}xz^2 + c_{17}z^2x + c_{18}zx^2 + c_{19}xyz + c_{20}x^4 + c_{21}y^4 + c_{22}z^4 + \\
 & c_{23}x^3y + c_{24}x^3z + c_{25}y^3z + c_{26}y^3z + c_{27}z^3y + c_{28}z^3x + c_{29}x^2y^2 + c_{30}y^2z^2 + c_{31}z^2x^2 + c_{32}x^2yz + \\
 & c_{33}y^2xz + c_{34}z^2xy + c_{35}x^5 + c_{36}y^5 + c_{37}z^5 + c_{38}x^4y + c_{39}x^4z + c_{40}y^4z + c_{41}y^4x + c_{42}z^4y + \\
 & c_{43}z^4x + c_{44}x^3y^2 + c_{45}x^2y^3 + c_{46}y^3z^2 + c_{47}y^2z^3 + c_{48}z^3x^2 + c_{49}z^2x^3 + c_{50}x^3yz + c_{51}y^3xz + \\
 & c_{52}z^3xy + c_{53}x^2y^2z + c_{54}x^2yz^2 + c_{55}y^2z^2x + c_{56}x^6 + c_{57}y^6 + c_{58}z^6 + c_{59}x^5y + c_{60}x^5z + \\
 & c_{61}y^5z + c_{62}y^5x + c_{63}z^5y + c_{64}z^5x + c_{65}x^4y^2 + c_{66}x^2y^4 + c_{67}y^4z^2 + c_{68}y^2z^4 + c_{69}z^4x^2 + \\
 & c_{70}z^2x^4 + c_{71}x^3y^3 + c_{72}x^3z^3 + c_{73}y^3z^3 + c_{74}x^4yz + c_{75}y^4xz + c_{76}z^4xy + c_{77}x^3y^2z + c_{78}x^3yz^2 + \\
 & c_{79}y^3z^2x + c_{80}y^3zx^2 + c_{81}z^3x^2y + c_{82}z^3xy^2 + c_{83}x^2y^2z^2 + c_{84}x^7 + c_{85}y^7 + c_{86}z^7 + c_{87}x^6y + \\
 & c_{88}x^6z + c_{89}x^4y^3 + c_{90}x^4z^3 + c_{91}x^3y^4 + c_{92}x^3z^4 + c_{93}x^2y^5 + c_{94}x^2z^5 + c_{95}xy^6 + c_{96}xz^6 + \\
 & c_{97}x^5y^2 + c_{98}x^5z^2 + c_{99}y^6z + c_{100}y^5z^2 + c_{101}y^4z^3 + c_{102}y^3z^4 + c_{103}y^2z^5 + c_{104}yz^6 + c_{105}x^5yz + \\
 & c_{106}x^4y^2z + c_{107}x^4yz^2 + c_{108}x^3y^3z + c_{109}x^3yz^3 + c_{110}x^3y^2z^2 + c_{111}x^2y^4z + c_{112}x^2yz^4 + \\
 & c_{113}x^2y^3z^2 + c_{114}x^2y^2z^3 + c_{115}xy^5z + c_{116}xy^4z^2 + c_{117}xy^3z^3 + c_{118}xy^2z^4 + c_{119}xyz^5 + \\
 & c_{120}x^8 + c_{121}y^8 + c_{122}z^8 + c_{123}x^7y + c_{124}x^7z + c_{125}x^6y^2 + c_{126}x^6z^2 + c_{127}x^5y^3 + c_{128}x^5z^3 + \\
 & c_{129}x^4y^4 + c_{130}x^4z^4 + c_{131}x^3y^5 + c_{132}x^3z^5 + c_{133}x^2y^6 + c_{134}x^2z^6 + c_{135}y^7z + c_{136}y^6z^2 + \\
 & c_{137}y^5z^3 + c_{138}y^4z^4 + c_{139}y^3z^5 + c_{140}y^2z^6 + c_{141}yz^7 + c_{142}xy^7c_{143}xz^7 + c_{144}x^6yz + c_{145}x^5y^2z + \\
 & c_{146}x^5yz^2 + c_{147}x^4y^3z + c_{148}x^4y^2z^2 + c_{149}x^4yz^3 + c_{150}x^3y^4z + c_{151}x^3y^3z^2 + c_{152}x^3y^2z^3 + \\
 & c_{153}x^3yz^4 + c_{154}x^2y^5z + c_{155}x^2y^4z^2 + c_{156}x^2y^3z^3 + c_{157}x^2y^2z^4 + c_{158}x^2yz^5 + c_{159}xy^6z + \\
 & c_{160}xy^5z^2 + c_{161}xy^4z^3 + c_{162}xy^3z^4 + c_{163}xy^2z^5 + c_{164}xyz^6 + c_{165}x^9 + c_{166}y^5 + c_{167}z^5 + \\
 & c_{168}x^8y + c_{169}x^8z + c_{170}x^7y^2 + c_{171}x^7z^2 + c_{172}x^6y^3 + c_{173}x^6z^3 + c_{174}x^5y^4 + c_{175}x^5z^5 + \\
 & c_{176}x^4y^5 + c_{177}x^4z^5 + c_{178}x^3y^6 + c_{179}x^3z^6 + c_{180}x^2y^7 + c_{181}x^2z^7 + c_{182}xy^8 + c_{183}xz^8 + \\
 & c_{184}y^8z + c_{185}y^7z^2 + c_{186}y^6z^3 + c_{187}y^5z^4 + c_{188}y^4z^5 + c_{189}y^3z^6 + c_{190}y^2z^7 + c_{191}yz^8 + \\
 & c_{192}x^6y^2z + c_{193}x^6yz^2 + c_{194}x^5y^3z + c_{195}x^5y^2z^2 + c_{196}x^5yz^3 + c_{197}x^4y^4z + c_{198}x^7yz + \\
 & c_{199}x^4y^3z^2 + c_{200}x^4y^2z^3 + c_{201}x^4y^1z^4 + c_{202}x^3y^5z + c_{203}x^3y^4z^2 + c_{204}x^3y^3z^3 + c_{205}x^3y^2z^4 + \\
 & c_{206}x^3yz^5 + c_{207}x^2y^6z + c_{208}x^2y^5z^2 + c_{209}x^2y^4z^3 + c_{210}x^2y^3z^4 + c_{211}x^2y^2z^5 + c_{212}x^2yz^6 + \\
 & c_{213}xy^7z + c_{214}xy^6z^2 + c_{215}xy^5z^3 + c_{216}xy^4z^4 + c_{217}xy^3z^5 + c_{218}xy^2z^6 + c_{219}xyz^7
 \end{aligned}$$

REFERENCES

1. Neuberger T. et al. // J. Magn. Magn. Mater. 2005. V. 293. P. 483.
2. Kuznetsov A. A. et al. // J. Magn. Magn. Mater. 1999. V. 194. P. 22.
3. Ruuge E. K., Rusetski A. N. // J. Magn. Magn. Mater. 1993. V. 122. P. 335.
4. Häfeli U. O., Pauer J. G. // J. Magn. Magn. Mater. 1999. V. 194. P. 76.
5. Ganguly R. et al. // J. Magn. Magn. Mater. 2005. V. 289. P. 331.
6. Voltairas P. A., Fotiadis D. I., Michalis L. K. // J. Biomech. 2002. V. 35. P. 813.